Spatiotemporal response described by the resonantly forced modified Korteweg–de Vries equation

L. G. Redekopp and Z. You
Department of Aerospace Engineering and Department of Mechanical Engineering, University of Southern California, Los Angeles, California 90089-1191
(Received 3 October 1994)

The wave field described by the cubic-nonlinear Korteweg–de Vries equation and stimulated by a source moving at transcritical speeds is examined by means of a numerical simulation. Depending on the source speed relative to the linear resonance condition, different upstream-propagating solitons appear, including waves of elevation, waves of depression, and breathers. Pairwise interactions of solitons are common.

PACS number(s): 47.10.+g, 47.20.Ky, 47.35.+i, 03.40.Kf

I. INTRODUCTION

The spatiotemporal response of nonlinear, dispersive wave systems subject to spatially confined forcings can exhibit a surprising composition of solution components, especially when the forcing occurs in the vicinity of a resonance of the linearized system. For example, the wave field defined by the Korteweg–de Vries (KdV) equation, when stimulated by a single compact disturbance which moves with a speed close to a limiting phase speed of the underlying linear operator, may give rise to a train of upstream-propagating solitons, multiple soliton-soliton interactions, stationary dimpled solitary waves of elevation or depression, slowly varying cnoidal wave trains, undular bores, dispersive lee waves, etc. [1–7]. When multiple or distributed forcings exist, a complex interaction of these solution components may occur on different time scales. In the present paper some of the multiplicity of solution components are reported for the modified Korteweg–de Vries (mKdV) equation when it is forced near resonance by a spatially isolated forcing effect.

The mKdV equation describes nonlinear wave motions in weakly dispersive systems where, because certain symmetry conditions of the media and boundary conditions comprising the waveguide are satisfied, the generic quadratic nonlinearity of the KdV equation vanishes identically. In these circumstances, the nonlinearity is of cubic order. A rather simple physical example where this occurs is interfacial gravity, or capillary-gravity, waves between two superposed, finite layers of immiscible fluids of different properties [8]. For a special combination of fluid densities and layer depths, the coefficient of the quadratic nonlinear term in an expansion valid for small, but finite, amplitude motions vanishes. Similar symmetry conditions can be found for other weakly dispersive systems (e.g., internal waves, Rossby waves, etc.). In such circumstances, the mKdV equation emerges as the leading-order balance equation for the evolution of long waves along a defining characteristic of the underlying linear operator.

II. PROBLEM DEFINITION

The mathematical model we study is the mKdV equation with a spatially distributed forcing taken in the form

$$v_t + U(t)v_x \pm \tfrac{3}{2}v^2 v_x - \tfrac{1}{6}v_{xxx} = \tfrac{1}{2}B'(x) \ . \tag{1}$$

This equation can be derived by a consistent asymptotic approximation in physical contexts and describes weakly nonlinear, weakly dispersive, plane waves generated by a distributed forcing, or source, defined by $B(x)$ when relative motion exists between the forcing and the media of the waveguide. A convenient physical context in which to discuss the dynamics described by (1) is that where a plane pulse of excess pressure $B(x)$ moves over a shallow liquid layer or, alternatively, where the liquid layer flows uniformly past a stationary deformation $B(x)$ in the bottom surface of the layer. We adopt the latter point of view in the present discussion with the coordinate x along the waveguide (liquid layer) and pointing in a direction downstream relative to the uniform motion of the media. The uniformly moving media has a speed close to a long-wave phase velocity of the dispersive system. In this way the upstream-propagating components of the disturbance field (i.e., those along the upstream characteristic) are resonant in that they cannot escape the continuous influence of the source $B(x)$, at least on a linear basis. The function $U(t)$ is a scaled deviation of the stream speed from the limiting long-wave phase velocity. In the application of a consistent asymptotic approximation leading to the derivation of the evolution equation (1) in any physical context, the deviatory transcritical speed $U(t)$ can vary on the same time scale as that for weakly nonlinear evolution along the upstream characteristic of the linearized system [5]. Hence (2) describes resonantly forced wave generation, including passage through resonance, in weakly dispersive systems where the nonlinearity is third order. When $U(t)$ is constant, the linear advection term of the homogeneous equation can be removed by a Galilean transformation. However, this is not useful for the inhomogeneous equation and we

prefer to study the equation where the forcing is fixed relative to the waveguide and the medium is in motion past the source. One may consider temporally varying forcing $B(x,t)$ in this reference frame, but this introduces additional time scales which are determined entirely by the source. The results reported here will focus almost entirely on the intrinsic dynamics associated with steady, transcritical forcing. In this case $U(t)$ will be a constant measuring whether the transcritical, steady forcing is supercritical ($U>0$) or subcritical ($U<0$). The discussion will close with one realization where $U(t)$ varies in the transcritical band.

The homogeneous or unforced version of (1) has several well-known solution components. When the nonlinear and dispersive terms have the same sign [the negative form of (1)], these effects compete and permanent wave forms are possible. Among these are a one-parameter family of single-crested solitons with either positive or negative polarity. These solutions, for the normalization used in the negative form of (1), have the form

$$v(x,t)=\pm\eta\,\mathrm{sech}\left\{\left[\frac{3}{2}\right]^{1/2}\eta\left[x+\frac{\eta^2}{4}t-x_0\right]\right\}$$
$$\equiv\pm v_s(x,t)\ . \tag{2}$$

These and the following solutions are presented for cases with vanishing deviatory transcritical speed $U(t)$. They can be extended to nonzero $U(t)$ by the transformation $x\to x-\int_0^t U(\tau)d\tau$. The solution components (2) derive from pure imaginary, discrete eigenvalues of the associated linear scattering problem arising in the inverse scattering transform (IST) for the solution of the homogeneous equation [9,10]. Both positive and negative polarities are possible for the negative form of (1) since a change in the sign of $v(x,t)$ leaves the homogeneous equation unchanged. However, the forced version precludes this freedom and the energy deposited in solitons with a given polarity will depend on the form of $B(x)$ as well as the initial condition. For this reason, and for later reference, we note that the volume (i.e., volume per unit span, or area) and energy of these solution components are, respectively,

$$\langle v_s\rangle\equiv\int_{-\infty}^{\infty}v_s(x,t)dx=(\tfrac{2}{3})^{1/2}\pi=2.565\ , \tag{3}$$

$$C_{1s}=\langle v_s^2\rangle\equiv\int_{-\infty}^{\infty}v_s^2(x,t)dx=\tfrac{2}{3}\sqrt{6}\eta\ . \tag{4}$$

The volume of these solitons is quantized and independent of the soliton amplitude, while their energy, which is the first of an infinite set of conserved densities, varies in direct proportion to the amplitude. Hence a zero-net-volume disturbance field can be composed of a soliton of each polarity, but each can have arbitrary amplitude. This is in stark contrast to the KdV equation having quadratic nonlinearity. In that case there is only one possible polarity of the soliton, which is determined by the sign of the nonlinear term. Furthermore, the volume of the wave is proportional to the amplitude and the wave cannot deform without gain or loss of volume. Hence the wave fields involving the soliton components of the solution set can be expected to be quite different for the KdV and mKdV equations with identical forcing. In fact, it will be shown later that solitons of the mKdV equation with both polarities can be generated by resonant forcing from a source $B(x)$, which has entirely positive or entirely negative volume.

Another family of soliton solutions of the homogeneous version of the negative form of (1) exist which are known as breather or bion states. These solutions are a two-parameter family and are fundamentally unsteady. They obtain from the existence of a pair of complex eigenvalues of the associated scattering problem in the IST satisfying the condition $\zeta=\xi+i\eta=-\zeta^*$, where the asterisk denotes the complex conjugate. This family of solutions, taking $U=0$, can be expressed in the alternate forms [9]

$$v(x,t)=\pm\frac{2}{3}\sqrt{6}\frac{\partial}{\partial x}\left\{\tan^{-1}\left[\frac{\eta}{\xi}\frac{\cos(\theta_2+\gamma)}{\cosh(\theta_1+\delta)}\right]\right\}$$
$$=\mp4\eta\xi\frac{\xi\cosh(\theta_1+\delta)\sin(\theta_2+\gamma)+\eta\sinh(\theta_1+\delta)\cos(\theta_2+\gamma)}{\xi^2\cosh^2(\theta_1+\delta)+\eta^2\cos^2(\theta_2+\gamma)}\equiv\pm v_b(x,t)\ , \tag{5}$$

where

$$\theta_1=\sqrt{6}\eta\{x+(\eta^2-3\xi^2)t\}\ ,$$
$$\theta_2=\sqrt{6}\xi\{x+(3\eta^2-\xi^2)t\}\ ,$$
$$e^{-\delta}=\frac{1}{2}\left|\frac{\xi}{\eta}\right|\frac{(A^2+B^2)^{1/2}}{(\xi^2+\eta^2)^{1/2}}\ ,\quad \tan\gamma=\frac{B\xi-A\eta}{A\xi+B\eta}\ .$$

The function θ_2 can be viewed as the carrier phase and θ_1 as the modulation phase, although these distinctions are not so useful when the wave numbers of the two phases are comparable. This family of solutions, in contrast to the family of single-crested solitons (2), has zero volume. They can be characterized by evaluating the first two conserved densities of the homogeneous equation [10],

$$C_{1b}=\int_{-\infty}^{\infty}v_b^2(x,t)dx=\tfrac{8}{3}\sqrt{6}\eta\ , \tag{6}$$

$$C_{2b}=\int_{-\infty}^{\infty}\{v_b^4+\tfrac{2}{3}v_b v_{bxx}\}dx=\tfrac{32}{9}\sqrt{6}\eta(\eta^2-3\xi^2)\ . \tag{7}$$

Evaluation of these conservation quantities for a given realization can yield the two independent parameters defining the breather state.

When the nonlinear and dispersive terms in the mKdV equation have opposite signs [i.e., the positive form of Eq. (1)], permanent wave solutions no longer exist. A variety of other analytical solutions of (1) can be constructed (e.g., cnoidal waves, stationary forced solitary waves,

similarity solutions, etc.), but they are not evident or do not have a clearly defined role in the numerical results reported here.

III. NUMERICAL RESULTS

Equation (1) was integrated numerically by a finite difference scheme. The equation was first integrated once with respect to the spatial coordinate to reduce the highest derivative to second order. The initial condition was a quiescent state with no forcing. At $t=0+$ the forcing was imposed centered at $x=0$ and the transient evolution in the domain $-L_1<x<L_2$ was computed. The equation was taken in the form

$$\frac{\partial H(x,t)}{\partial t}=G(x,t)\ ,\quad H(x,t)=\int_{-\infty}^{x} v(y,t)dy\ ,$$
$$G(X,t)=-Uv\mp\tfrac{1}{2}v^3+\tfrac{1}{6}vxx+\tfrac{1}{2}B(x)\ . \tag{8}$$

The integral was computed by the trapezoidal rule and the spatial derivative was evaluated using a central difference. A predictor-corrector method was used to advance in time, yielding a second-order accuracy in space and time. Radiation boundary conditions were applied at both ends of the spatial domain to allow waves to escape with minimum reflection, but the length of the spatial interval L_1 was almost always chosen sufficiently large to capture the upstream response for the entire integration time. The numerical simulation was validated by solving the KdV equation and reproducing the results of Fornberg and Whitham [11]. Initial conditions were selected consisting of three solitons with amplitudes chosen such that two pairwise interactions occurred in an interval of 125 spatial units. The integration time was 400 units with the largest wave propagating over 225 units. The conserved density C_1 was computed and found to have a loss of no more than one-half of a percent. Amplitude ratios of the solitons in initial conditions were chosen to encompass the three different classes of soliton interactions defined by Lax [12]. The maximum error in the phase shift was one-eighth of a wavelength of the largest wave after it propagated over 20 wavelengths and experienced two pairwise interactions. This provided confidence that the numerical simulations were faithfully describing the qualitative and quantitative character of the true solution.

A sequence of numerical simulations was performed for an isolated forcing of the form

$$B(x)=B_0 e^{-(x/x_0)^2}\ . \tag{9}$$

The parameter B_0 measures the strength and sign of the forcing and x_0 the spatial scale of the forcing. The present study is focused on the nature of the upstream disturbance field that appears under different transcritical conditions, especially the possible generation of solitons of different polarities and breather states, rather than on an exhaustive study of the effect of different forcing disturbances. For this reason the forcing parameters are fixed at $B_0=1.15$ and $x_0=0.4$. One should note that change in the sign of B_0 is equivalent to a change in the sign of $v(x,t)$, leaving Eq. (2) unchanged. Hence a change in the sign of the forcing will lead, for example, to a change in the polarity of soliton states.

A useful diagnostic of the computed solution is the quantity $D(t)$ defined by

$$D(t)=\int_{-\infty}^{\infty} v(y,t)B'(y)dy=\frac{dC_1}{dt}\ . \tag{10}$$

In a fluid-dynamical context, this represents the drag force acting on the (topographic) forcing disturbance in the waveguide. The function is quite useful in defining the periodicity, or aperiodicity, of the resonant response and the onset of a symmetric, supercritical state. It also provides good insight to the temporal dynamics of the solution field in the immediate vicinity of the forcing or generating source.

A. Results for steady forcing

The spatiotemporal response was computed for a sequence of transcritical conditions using the negative form of Eq. (1). Figure 1 shows a rastor plot of the solution field and a time history of the drag force for a simulation with $U=-0.3$. After an initial transient phase, a trapped, (essentially) periodic response occurs for this slightly subcritical forcing. The first two conserved densities were computed to ascertain whether the computed behavior corresponded to a stationary breather. Both C_1

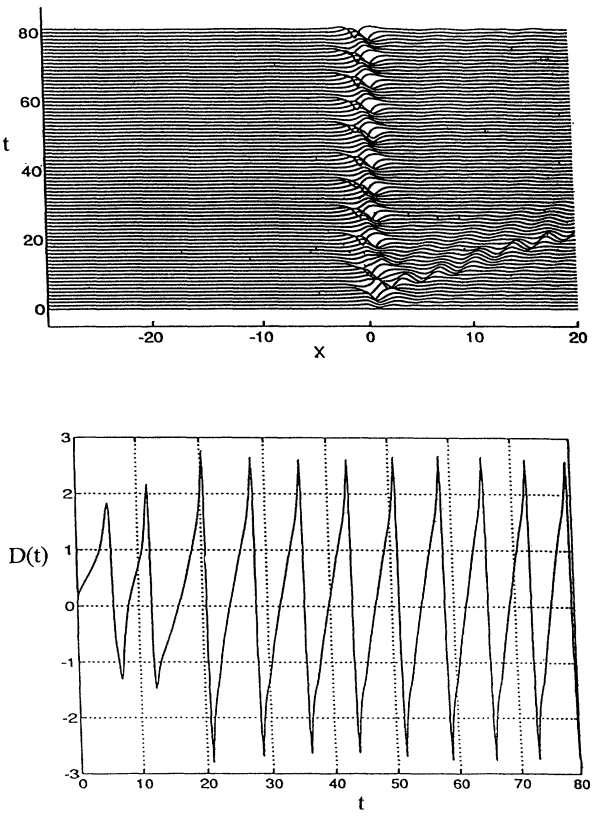

FIG. 1. Solution field and drag force history for steady forcing with transcritical speed $U=-0.3$.

and C_2 were found to be time dependent. Hence the trapped stationary response is not a standing breather. The function $D(t)$ exhibits a character reminiscent of relaxation oscillations with strong reversals from positive to negative values, followed by slower buildup again to positive values of the drag force. The simulation reveals a complete absence of any upstream response and a weak, but definitely not vanishing, lee-wave response. The lee-wave response is very small compared to the stationary or trapped response.

When the transcritical velocity is increased, the period of the trapped response increases and, eventually, upstream-propagating breathers are born. This is shown in Fig. 2 for the condition $U=0.1$. They were also observed in simulations at $U=-0.2$ and 0, but only one breather was captured in simulations limited to $t<80$. The simulation for $U=0.1$ shown in Fig. 2 was not continued for a sufficiently long time to ascertain whether this emission of runaway breathers occurred periodically, but indications from the rastor plot are suggestive that this is the case. The simulation was initially stopped at a time $t=70$, but later restarted to gain a better representation of the second breather. The latter simulation was then discontinued at the last trace on the figure because of the appearance of numerical instabilities in the lee of the forcing, most likely stimulated from higher wave number disturbances exiting via the outflow boundary condition. In the restart of the simulation at $t=70$, small errors led to a slightly increased speed of the lead breather. Evaluation of the conserved densities when each wave was centered around the position $x=-10$ gave $C_{1b}^{(1)}=7.11$ for the lead wave and $C_{1b}^{(2)}=6.99$ for the second wave. Computation of the second conserved density for each soliton yielded the values $C_{2b}^{(1)}=6.08$ and $C_{2b}^{(2)}=5.81$. From these values we obtain the pairs $(\eta_b^{(1)},\xi_b^{(1)})=(1.09,0.43)$ and $(\eta_b^{(2)},\xi_b^{(2)})=(1.07,0.42)$. Although these differences are significant, limited resources precluded further pursuit of the periodic nature, or lack thereof, of the response. Nevertheless, we believe that the asymptotic response at this transcritical condition consists of a periodic generation of upstream-propagating breathers.

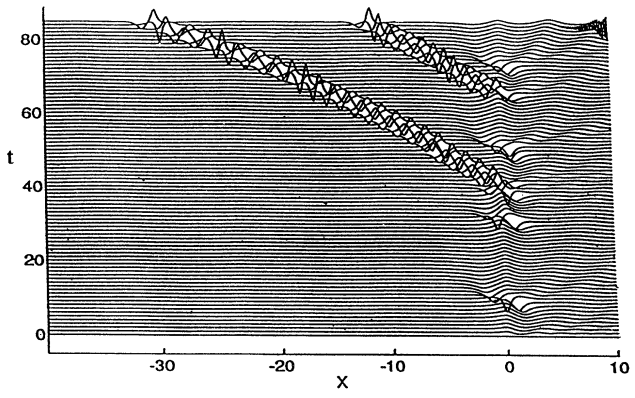

FIG. 2. Solution field for steady forcing with transcritical speed $U=0.1$.

As the transcritical speed is increased further, a quite complex wave field in the upstream region emerges in which breathers plus single-humped solitons of both polarities, and their mutual interactions, appear. The wave field for $U=0.208$ containing all these components is shown in Fig. 3. Figure 3(a) shows the "early" history of the simulation where all three forms of solitons are evident. In order to pursue the "asymptotic" nature of the response without extending the spatial interval, the far-upstream field was suppressed at a time ($t=120$) when its effect on the dynamics in the vicinity of the forcing region would have been minimal and the simulation was continued. The results are shown in Fig. 3(b). It appears that the breathers are limited to the earlier portion of the

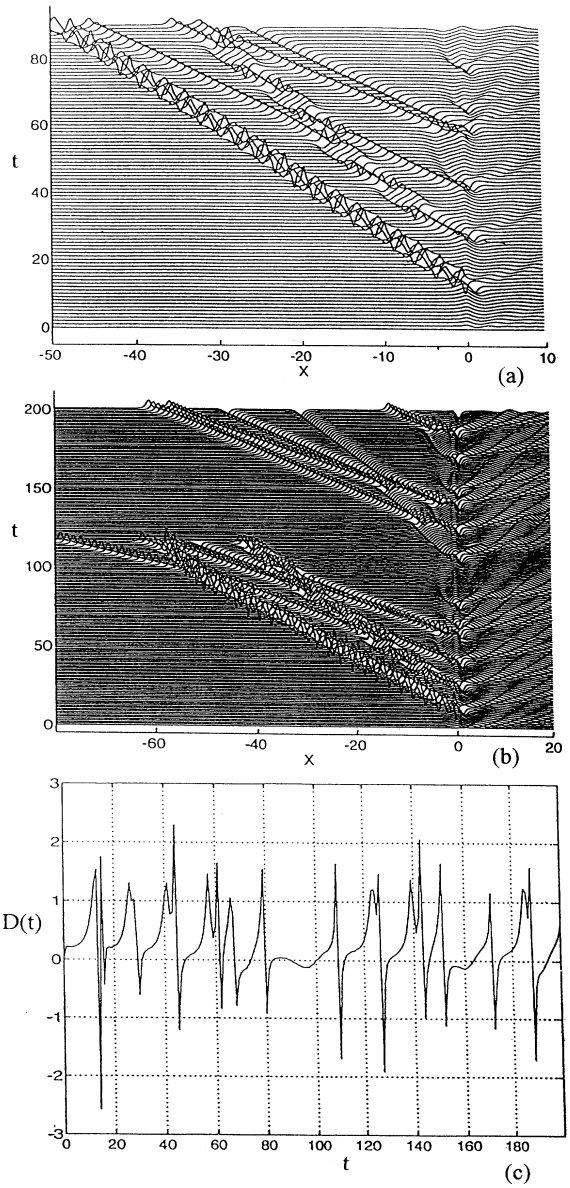

FIG. 3. Solution field for steady forcing with transcritical speed $U=0.208$. (a) Early time history; (b) extended time history; (c) drag history.

simulation. Their generation may be part of the transient adjustment phase following the impulsive switching on of the forcing function $B(x)$ and the true "periodic element" in the upstream wave field is that captured for times in the approximate interval $110 < t < 170$. Of course, there are no *a priori* reasons why the upstream response in the asymptotic state should be periodic. The drag history in Fig. 3(c) is quite irregular with strong and sudden jumps from positive to negative values during the emission of an upstream-propagating component. It is also clear that the development of these sudden transitions is also accompanied by the generation of a dispersive lee-wave packet. The wave forms associated with the two leading breathers are captured in the spatial structures $v(x,t_i)$ at successive time intervals in Fig. 4. The lead breather has essentially completed one period of its "carrier" phase in this interval of four units. Using the relations for the two conserved densities (6) and (7), the results in Table I are obtained. Based on these results, the predicted period for the lead breather is $T=3.8$.

It is interesting to compare the results for the negative form of (1) with $U=0.208$ in Fig. 3 to the response of the positive form of (1) under the same conditions. In this case a completely supercritical response appears, after an initial transient consisting of a dispersive lee-wave packet, characterized by a single wave of elevation centered directly above the forcing bump and having a shape closely approximating the symmetric bump. The drag history is shown in Fig. 5, where it is apparent that he response, after the transient, is entirely symmetric yielding zero drag.

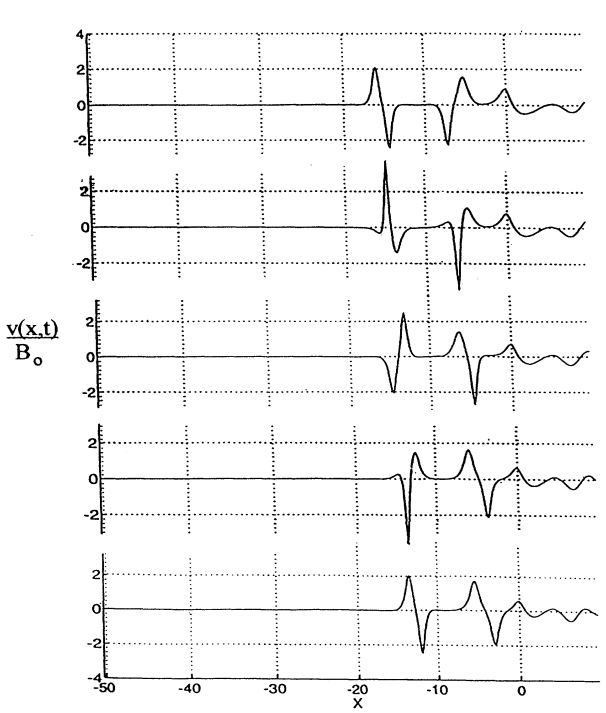

FIG. 4. Wave forms covering approximately one period of the lead breather shown in Fig. 3 (profiles taken at $t=34-38$, successively from top to bottom).

TABLE I. Breather soliton parameters for the waves shown in Fig. 4.

Wave	C_1	C_2	η	ξ
First breather	6.55	6.75	1.00	0.27
Second breather	5.73	5.58	0.88	0.12

Returning to the integration of the negative form of (1), Figs. 6 and 7 show the response for transcritical speeds $U=0.3$ and 0.4, respectively. At $U=0.3$, breathers no longer appear, but a periodic generation of upstream-propagating single-crested solitons with both polarities occurs. The response during one period is characterized by a soliton of elevation followed closely by a soliton of depression. Apparently, the lack of generation of a breather state is related to the time interval separating the pairwise formation of solitons of elevation and depression. Computation of the volume of the lead pair gives $\langle v_b^{(1)} \rangle_e = 2.54$ and $\langle v_b^{(1)} \rangle_d = 2.52$ for the wave of elevation and depression, respectively. These values compare very favorably with the quantization value given in Eq. (3). In fact, these numerical values were obtained from the response computed at $t=50$ for which the wave of elevation had already experienced a pairwise interaction with the second solitary wave of elevation as shown at the top of Fig. 6. At this time, the volume of the second soliton of elevation is $\langle v_b^{(2)} \rangle_e = 2.53$. Computation of the conserved density C_{1s} [cf. Eq. (4)] for these waves at $t=50$ gives the values $C_{1se}^{(1)}=3.70$, $C_{1sd}^{(1)}=2.43$, and $C_{1se}^{(2)}=3.71$. The values for the two waves of elevation are very similar, reinforcing the conclusion that the steady forcing has yielded a periodic temporal response. These results clearly yield $\eta_{se}^{(1)} > \eta_{sd}^{(1)}$ so that the waves of elevation have a greater phase speed than the waves of depression. Hence the asymptotic upstream state at this forcing condition will contain a discrete infinity of pairwise soliton interactions between waves of elevation and waves of depression. With the phase shifts accompanying each pairwise interaction, one can anticipate forcing conditions when triplet interactions occur, but we did not explore the parameter space to obtain a realization of such a state. Examination of the drag history reveals that the generation of a wave of elevation coincides with a locally increased drag force, while the generation of a wave of depression is associated with a stronger, concentrated reversal in the drag force. In a fluid-dynamical context,

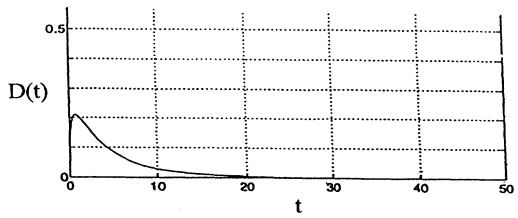

FIG. 5. Drag history of nonlinear dispersive case [positive form of (1)] under steady forcing with transcritical speed $U=0.208$.

the drag reversal would be expected to yield locally strong decelerations and flow separation, conditions which could give rise to strong events for scouring of the surface and possible suspension of particulates. A data set showing this power of the unsteady flow field associated with the generation and upstream propagation of internal solitary waves of elevation in shallow waters off the coast of California has been obtained recently [13].

When the transcritical speed is increased to $U=0.4$ for the chosen, fixed forcing function, the generation of solitons of depression has vanished and a periodic generation consisting only of waves of elevation appears in the upstream field (cf. Fig. 7). Computation of the volume of both waves gives the common value 2.54. The first conserved density C_1 agrees, to four significant figures, with the common value of 3.986, for both solitons. The drag force is always positive with concentrated peaks centered around the soliton-generation times. The dispersive, downstream-propagating portion of the solution field becomes weaker as the transcritical speed increases and, when comparing Figs. 6 and 7, is also weaker when upstream-propagating solitons of elevation are generated as opposed to the generation of solitons of depression. It appears that the lead soliton of elevation, when followed

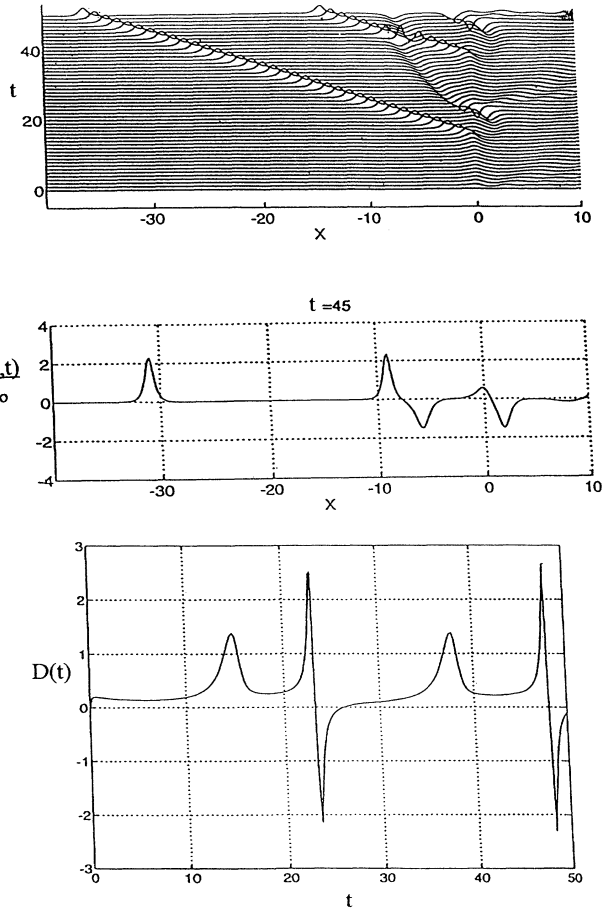

FIG. 6. Solution field and drag force history for steady forcing with transcritical speed $U=0.3$.

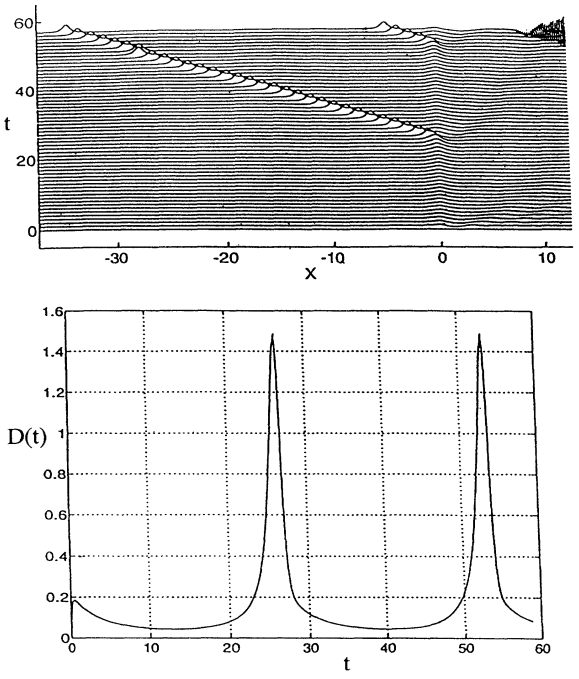

FIG. 7. Solution field and drag force history for steady forcing with transcritical speed $U=0.4$.

by a soliton of depression, has a strong compensating valley on the lee side of the forcing. This valley is less pronounced when solitons of depression no longer appear at higher transcritical speeds.

At higher values of the transcritical speed the period of soliton generation increases rapidly toward infinity and the dispersive tails become weaker. At $U=0.5$ a completely supercritical state is reached. After a short transient, the drag force vanishes and a stationary, single-crested, symmetric response centered on the forcing appears whose amplitude decreases as the speed U is increased further.

B. Results for unsteady forcing

The simulations presented above all involved steady flow over a stationary, fixed forcing. Clearly, a variety of unsteady cases could be posed. We present here a single unsteady realization for the negative form of (1) as a basis for revealing the kind of localized events that may occur. We consider a case with time-varying flow speed where $U(t)$ relaxes continuously from a supercritical speed into the transcritical regime and then accelerates back to the original supercritical speed. During any unsteady motion, several competitions occur which determine the spatiotemporal response. First, the residence time in the transcritical region, relative to the soliton-generation times at any transcritical speed, will determine the energy deposited into the upstream wave field. Second, the depth of relaxation below the supercritical-transcritical boundary determines the type of upstream solitons (i.e., waves of elevation, depression, or breathers)

which can appear. The steady results shown above reveal that breathers are found for forcing near the subcritical-transcritical boundary and only solitons of elevation appear near the supercritical-transcritical boundary. Hence the nature of the upstream response depends quite crucially on the trajectory of $U(t)$ through and in the transcritical region.

The realization presented here is for the same forcing $B(x)$ used in all previous simulations and with the transcritical trajectory

$$U(t)=\tfrac{1}{2}-\tfrac{1}{2}\mathrm{sech}^2\{\tfrac{2}{5}(t-30)\}\ , \tag{11}$$

which is symmetrically centered about the time $t=30$. The trajectory $U(t)$ relaxes from the supercritical speed $U=\frac{1}{2}$ down to $U=0$ at $t=30$ and then returns to $U=\frac{1}{2}$. The central time $t=30$ was chosen so that any initial transients in the supercritical response at $U=\frac{1}{2}$ would have radiated away before the trajectory entered the transcritical region. The depth of relaxation was chosen to be significantly below the threshold value above which no breathers were found under steady conditions. The computed spatiotemporal response is exhibited in Fig. 8.

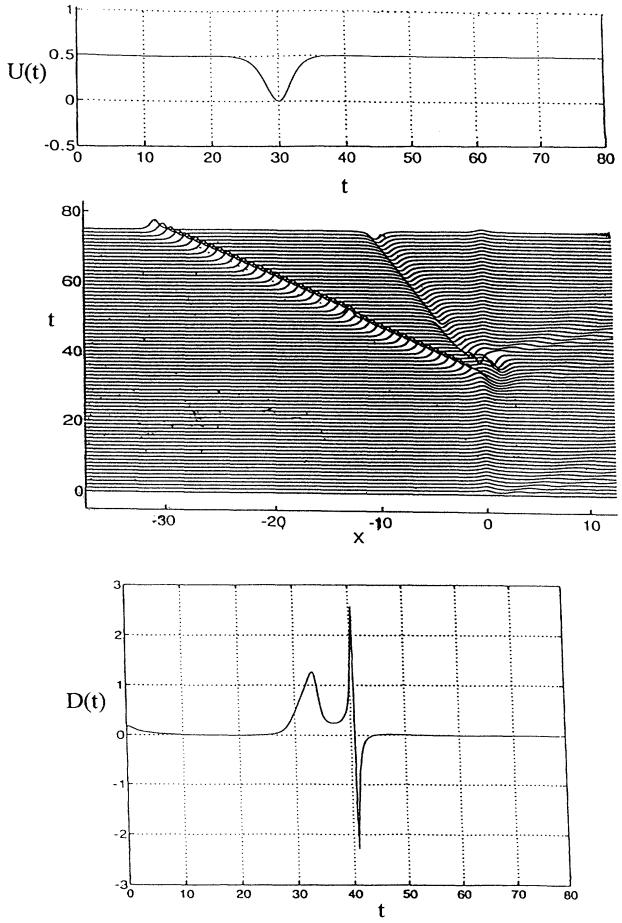

FIG. 8. Solution field and drag force history for an unsteady trajectory in the transcritical region [cf. Eq. (11)].

The quiescent, supercritical state with zero drag preceding and following the transcritical excursion is evident. The upstream response during the transcritical excursion consists of a pair of solitons, a lead one of elevation followed by one of depression. The lead wave of elevation has a volume of 2.54 while the wave of depression has an almost identical negative volume of -2.55. The first conserved density for the two waves, respectively, is 3.61 and 2.83, consistent with the fact that the wave of depression has a slower phase speed than the wave of elevation. The forced generation of these solitons has a concomitant generation of a dispersive packet which radiates downstream from the forcing. The drag force history shows the characteristic sharp reversal associated with the generation of the soliton of depression. It is evident that the competition between the soliton generation time scales and the residence time in certain portions of the transcritical band has precluded the generation of any breather states. An extended sample of trajectories could be examined, but the present results provide a good understanding of the main qualitative features of the resonantly forced mKdV equation. Further simulations should probably be motivated by specific applications.

IV. CONCLUDING REMARKS

The KdV equation with cubic nonlinearity has been examined by means of numerical simulation for conditions when a spatially localized forcing disturbance moves with transcritical speeds relative to the limiting phase speed of the underlying dispersive system. The unbounded resonant response of the linear system is avoided by nonlinear and dispersive competitions. When nonlinearity and dispersion are in direct competition, the resonant response involves the generation of upstream-propagating solitons in a manner reminiscent of the resonantly forced KdV equation. In contrast with the KdV equation, however, the mKdV equation admits three different soliton states and all three have been found in the upstream wave field under certain forcing conditions. This work identifies all three soliton states in a particular spatiotemporal realization. Under some forcing conditions, only one or two of the soliton states are found to exist. When nonlinearity and dispersion act in unison, no soliton states exist and the upstream field is quiescent for all parameter conditions studied.

The present work has explored only a small subset of conceivable transcritical forcing scenarios. Nevertheless, the simulations reported here do provide a good qualitative understanding of the nature and composition of the complex upstream wave field that can be expected. This wave field can contain, in addition to isolated solitons, interactions of solitons with locally strong accelerations and decelerations. Furthermore, the generation of breathers and solitons of depression is accompanied by strong and sudden reversals in the drag force acting on the generating source. In some waveguides, such as internal waves in a shallow layer, the physical conse-

quences of these strongly unsteady events at the generating source, or locally where solitons collide, may be profound. Other scenarios with multiple forcing sites can give rise to local confluences of unsteady events with complex dynamics. In such cases, the implications for physical processes will be even greater.

ACKNOWLEDGMENTS

Partial support was received from the Office of Naval Research under Contract No. N00014-92-J-1062. Some of the computer time was provided by the San Diego Supercomputer Center.

[1] T. R. Akylas, J. Fluid Mech. **141**, 455 (1984).
[2] T. Y.-T. Wu, J. Fluid Mech. **184**, 75 (1987).
[3] R. H. J. Grimshaw and N. Smyth, J. Fluid Mech. **169**, 429 (1986).
[4] S. J. Lee, G. T. Yates, and T. Y.-T. Wu, J. Fluid Mech. **199**, 569 (1989).
[5] V. D. Djordjevic and L. G. Redekopp, Wave Motion **15**, 1 (1992).
[6] L. G. Redekopp and Z. You, Bull. Am. Phys. Soc. **37**, 1809 (1992) and (unpublished).
[7] J. Kevorkian and J. Yu, J. Fluid Mech. **204**, 31 (1989).
[8] L. G. Redekopp, *Fluid Dynamics in Astrophysics and Geophysics,* edited by N. R. Lebovitz, Lectures in Applied Mathematics Vol. 20 (American Mathematical Society, Providence, RI, 1983), pp. 59–78.
[9] M. Wadati, J. Phys. Soc. J. **34**, 1289 (1973).
[10] M. J. Ablowitz and H. Segur, *Solitons and the Inverse Scattering Transform* (SIAM, Philadelphia, 1981).
[11] B. Fornberg and G. B. Whitham, Proc. R. Soc. London Ser. A **289**, 373 (1978).
[12] P. Lax, Comments Pure Appl. Math. **21**, 467 (1968).
[13] D. Bogucki, T. D. Dickey, and L. G. Redekopp (unpublished).